APPLICATION OF OPEN CIRCUIT VOLTAGE DECAY TO THE CHARACTERIZATION OF p/n$^+$ AND n/p$^+$ EPITAXIAL LAYER

M. Ťapajna*, J. Pjenčák, A. Vrbický, P. Kúdela, L. Harmatha

Department of Microelectronics, Faculty of Electrical Engineering and Information Technology, Slovak University of Technology, Ilkovičova 3, 812 19 Bratislava, Slovak Republic

Summary High quality silicon epitaxial layers are inevitable in bipolar and/or unipolar technology. However, its properties are not as easy characterized as those of bulk material. The recombination lifetime is dominated by surface/interface recombination for thin layers, which epitaxial ones generally are. We have designed diode structure with n$^+$n/p$^+$ and p$^+$p/n$^+$ epitaxial layer for open circuit voltage decay (OCVD) technique. In such a structure, injected carriers are constrained within lightly doped base by potential barriers of junction and high-low contact and their concentration can then decrease only by recombination. Carrier lifetime obtained by this manner yields information mainly about the defect properties of epitaxial layer. Performing OCVD measurement for high-level injection condition, also τ_n and τ_p could be evaluated.

1. INTRODUCTION

The open-circuit voltage decay (OCVD) technique was one of the earliest method for carrier lifetime determination [1]. It is easy to implement and interpretation of experimental data is fairly straightforward, moreover it is expected very good correlation to real electrical parameters of devices. In this method, a diode is forward biased and a steady-state excess carrier is established in lightly doped region. Once, the diode bias circuit is opened and subsequent excess carrier recombination is detected by monitoring open circuit voltage. High-injection and low-injection lifetimes are then evaluated from two distinct regions of voltage transient respectively.

In bipolar and unipolar technology, epitaxial (epi) layers are routinely used because they contain fewer metallic contaminants and lower oxygen densities than bulk Cz wafers. The quality of these layers could be evaluated with recombination or generation lifetime measurement in some way [2, 3]. However, there may arise some uncertainty in lifetime measurement due to fact, that epi layers are generally thinner than minority carrier diffusion length, forasmuch as OCVD method (alike the most commonly used techniques) measure the recombination lifetime.

Parameter obtained in this manner yield more information about the surface and epitaxial layer/substrate interface than about the epi layer itself. Nevertheless, this difficulty can be overcomes by growing of an epi layer with counter doping type than the substrate, *i.e.* making of np$^+$ or pn$^+$ junction respectively and subsequent creation of high-low contact with diffusion or epitaxial growth with higher doping concentration (Fig. 1). This structure affect as the effective potential barrier for constraining of injected carriers within the lightly doped region, which can decrease with time only through electron-hole recombination. When the high-low contact is grown in one technological step with epi layer *e.g.* by extending the impurity flow or using diffusion process, it is expected high-quality n$^+$/n or p$^+$/p interface respectively, with negligible low recombination velocity, hence, recombination lifetime is mostly influenced by bulk of lightly doped epi layer. Moreover, as will be mentioned in section 2, the width of lightly doped region should be less than an ambipolar diffusion length, thereby this structure is suitable for thin epi layer characterization.

In this paper, we have analyzed n$^+$np$^+$ and p$^+$pn$^+$ structures respectively, using both epi growth and diffusion for high-low contact preparation. Lifetime obtained from OCVD response using such a structures has been discussed according to experimental as well as simulated *I-V* characteristics.

2. THEORETICAL BACKGROUND

In this section, we consider structure as those in figure 2.a) with short base width. The recombination lifetime is determined by three main recombination mechanisms: Shockley-Read-Hall (SRH) or multiphonon recombination characterized by the lifetime τ_{SRH}, radiative recombination characterized by τ_{rad} and Auger recombination τ_{Auger} according to relationship [4]

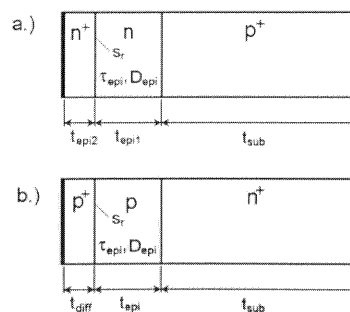

Fig. 1. Samples geometry for n$^+$np$^+$ and p$^+$pn$^+$ structures.

* Corresponding author. Tel.: + 421-2 602 91 872. *E-mail address:* milan.tapajna@stuba.sk

$$\tau_r = \frac{1}{\tau_{SRH}^{-1} + \tau_{rad}^{-1} + \tau_{Auger}^{-1}} . \quad (1)$$

Since Si is indirect band-gap semiconductor, radiative recombination plays almost no role, moreover, the Auger effect can be neglect when current density remains below 100 A/cm^2 [5], as shown below (see section 3), this condition will be fully satisfied. On the basis of this assumption, the recombination lifetime is controlled by SRH mechanism given by [4]

$$\tau_r \cong \tau_{SRH} = \frac{\tau_p(n_0 + n_1 + \Delta p) + \tau_n(p_0 + p_1 + \Delta p)}{p_0 + n_0 + \Delta p} . \quad (2)$$

where only one dominant recombination center is considered and n_1, p_1, τ_n and τ_p are defined as

$$n_1 = n_i \exp\left(\frac{(E_T - E_i)}{kT}\right), p_1 = n_i \exp\left(\frac{(E_i - E_T)}{kT}\right) . \quad (3)$$

$$\tau_p = \frac{1}{\sigma_p v_{th} N_T}, \qquad \tau_n = \frac{1}{\sigma_n v_{th} N_T} . \quad (4)$$

Here, n_0 and p_0 and Δp are equilibrium or the excess minority carrier density respectively, E_T is the trap energy level in the band-gap, E_i is the Fermi intrinsic energy level, $\sigma_{p,n}$ is the electron and hole capture cross section respectively, v_{th} is the thermal velocity and N_T is density of impurities.

Equation (2) simplifies for both low-level and high-level carrier injection. Under low-level condition, when the excess minority carrier density is low compared to the equilibrium majority carrier concentration $\Delta p << n_0$, recombination lifetime becomes

$$\tau_r(ll) \approx \tau_p\left(1 + \frac{n_1}{n_0}\right) + \tau_n \frac{p_1}{n_0} \cong \tau_p . \quad (5)$$

where the second approximation is assumed, $n_1 << n_0$ and $p_1 << n_0$.

Similarly, for high-level condition, when holds the inequality $\Delta p >> n_0$ one gets expression

$$\tau_r(hl) \approx \tau_p + \tau_n . \quad (6)$$

Performing OCVD measurement under high-level condition, one should use sufficiently large forward current during initial pulse. Then, for structure such as those at Fig. 1 it is possible to estimate the high-level carrier lifetime from the linear part of the open voltage as [6]

$$\tau_r(hl) = -2kT/q(dV/dt)^{-1} . \quad (7)$$

Under low-level condition, inequalities $\Delta p >> p_0$ and $\Delta n << n_0$ holds. Total open circuit voltage is equal only to voltage across p$^+$n $V = V_{j1}$. Excess carrier concentration is then given by

$$\Delta p = p_0\left[\exp(qV/kT) - 1\right] . \quad (8)$$

Considering an idealized situation, where the carrier trapping and surface effect can be neglect, and assuming total voltage to be much larger than kT/q, low-level lifetime is given [6]

$$\tau_r(ll) = -kT/q(dV/dt)^{-1} . \quad (9)$$

2.1. Surface and interface recombination

Recombination process during OCVD transient in samples shown in Fig. 1 is not affected only by bulk recombination but it is given either by lateral surface recombination and interface recombination at the high-low contact. Unlike usually used structures [3], in our configuration, only one interface contributes to entire recombination on the assumption that carrier trapping is neglected. Although the interface recombination velocity s_r of a high-low junction tends to be low, it could has significant influence to measured lifetime especially when epi layer lifetime τ_{epi} is on the order of several hundreds μs, what is really the case in today's state of technology. Therefore, it is convenient to define effective lifetime τ_{reff}, which can be written as [7]

$$\frac{1}{\tau_{reff}} = \frac{1}{\tau_{epi}} + \frac{1}{\tau_s} = \frac{1}{\tau_{epi}} + D_{epi}\beta^2 , \quad (10)$$

where τ_s is the surface/interface lifetime, D_{epi}, t_{epi} is diffusion coefficient and thickness of epi layer, respectively and the parameter β is determined from the implicit equation

$$\cot(\beta t_{epi}) = \frac{\beta D_{epi}}{s_r} . \quad (11)$$

Separation of surface recombination component is quit difficult. Nevertheless, we will discuss this issue more detailed in section 3.

Influence of lateral surface recombination is illustrated in Fig. 3 on the curve b.) (dashed line). Such a transient was recorded immediately after sample separation by wafer cleaving. However, this effect could be sufficiently suppress by performing edge etching, moreover, for the large diameter of the diode used in collecting experimental data, perimeter recombination can be neglect, when the effective lifetime remains below 10^{-3} s [4].

3. EXPERIMENT AND RESULTS

The circuit arrangement used for OCVD measurement comprised of Lifetime Test Unit OCD-2B, which contain power supply and fast transistor switch. The open circuit voltage decay was monitored by Tektronix TDS3000B digital oscilloscope and *I-V* characteristics of the diodes under study were recorded using Keithley 237 Source Meter. For simulation, commercial software ISE TCAD 9.0 was used.

To cover both p-type as well as n-type epi layers characterization, two series of samples were fabricated, denotes as D01 and D02. Sample D01 was prepared on the <111>-oriented p-type boron doped 525 μm thick substrate with concentration of 3.24×10^{18}–1.34×10^{19} cm^{-3}. Two n-type epi layers were grown step by step with phosphorous doping. The first one has concentration of 2×10^{14} cm^{-3} and at the second one with thickness of ~5 μm, phosphorous concentration was increased by two

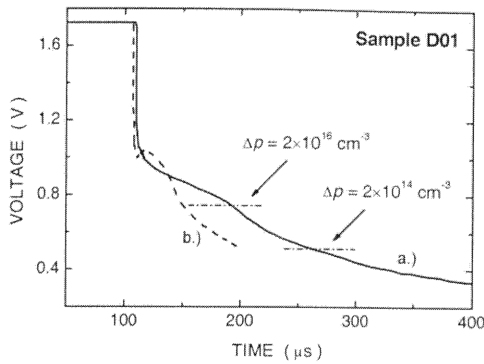

Fig. 2. OCVD response of sample D01.

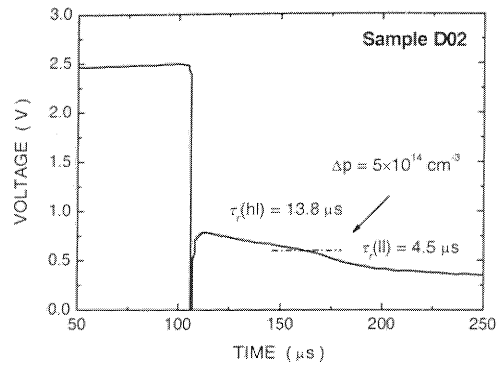

Fig. 3. OCVD response of sample D02.

orders. The resulting base thickness was approximately 55 μm.

Sample D02 was prepared on the <111>-oriented n-type phosphorous doped 375 μm thick substrate with concentration higher than 6.6×10^{18} cm^{-3}. P-type epi layer was grown with boron concentration of 5×10^{14} cm^{-3} but unlike D01, high-low junction was created by boron diffusion. The resulting base width of sample D02 was similar to those of D01. AlSiCu contacts were prepared by ions sputtering (a thickness 1.5 μm) and after that, wafers were cleaving to periodical hexagons (with area 19.1 mm^2). Prior to plasma etching of samples edges, they were partially packaged.

Fig. 3 shows typical OCVD response of the sample D01 (curve a.) drawn by solid line) and as was mentioned above, voltage transient influenced by high lateral recombination surface velocity (curve b.)) is also reported. It is clearly demonstrate, that lateral recombination is effectively suppressed, because it affects both, transient shortening and its shape as well, but the shape of curve a.) is quite different, thereafter we suppose lateral contribution to be insignificant.

At Fig. 3a.) transient, two regions could be distinguished, which represent typical OCVD for high-level (herein 140 – 180 μs) and subsequent

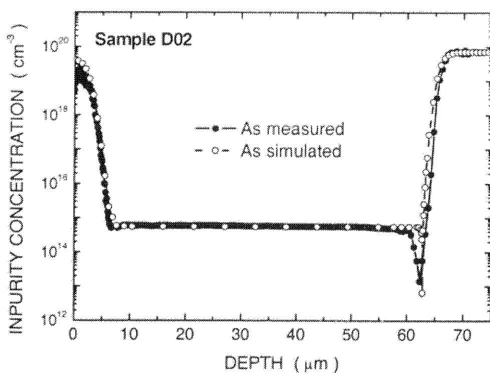

Fig. 4. Experimental (SRP) and simulated impurity depth profile of sample D02.

low-level (190 – 215 μs) lifetime measurement. However, from the conversion of voltage curve into the excess carrier density transient by equation

$$[\Delta p + p_0][\Delta p + n_0] = n_i^2 \exp(qV/kT), \qquad (12)$$

(concentrations are labeled by horizontal dash-dot line in Fig. 2) one can see, that at t=193 μs minority excess carriers decrease only below majority concentration in n$^+$ emitter and they decrease under base majority concentration as far as t=260 μs. Hence, at the earlier part of the voltage decay, diode behaves as an Rnp$^+$ structure (R denotes ohmic contact with infinite recombination rate). Effective lifetime obtained from this transient could leads to misinterpretation, nevertheless, providing appropriate analysis, correct value of the lifetime could be obtained [8].

Typical OCVD response of the structure D02 is shown in Fig. 3. Unlike sample D01, high-low junction of the diode D02 was prepared by diffusion with p$^+$ concentration of three orders above the epi p base doping, which is accomplish at depth profile obtained from spreading resistance profiling measurement and simulation of technological process (Fig. 4). Using eqn. (12) again, excess carrier concentration was determined and compared with base doping, which is labeled by dash-dot line in Fig. 3. Here, the value of injected carrier correlates well with transition between high to low-level injection, thereafter, proper lifetimes could be determined. From the fitting of distinct regions at the curve, it was extracted as τ_r(hl)=13,8 μs and τ_r(ll)=4,5 μs and according to equations (5) and (6) one can obtain carrier lifetimes τ_n=4,5 μs and τ_p=9,3 μs, respectively.

In order to verify obtained value of recombination lifetime, we realized procedure for τ_r and τ_g (generation lifetime) determination proposed by Poyai *et. al.* [9] based on extraction of recombination current from forward *I-V* and *C-V* measurement. It should be noted, that since our diodes have sufficiently large area, we did not separate perimeter and bulk current density.

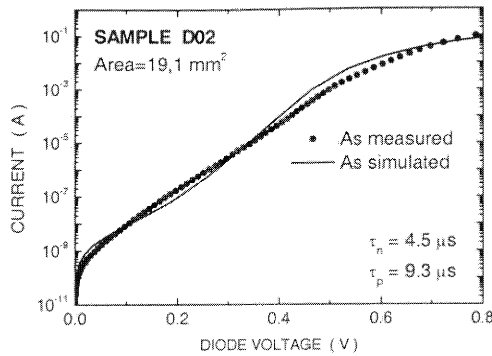

Fig. 5. Experimental and simulated I-V characteristic of sample D02.

Experimental *I-V* characteristic of diode D02 is shown at the Fig. 5, from here we derived diffusion current density as J_{d0}=80 pA. Forasmuch diode current density can be written as

$$J=\left[J_{d0}+\frac{qn_i w}{2\tau_r \exp(qV/2kT)+\tau_g}\right]\left[\exp\left(\frac{qV_t}{kT}\right)-1\right],$$

where w ($=\varepsilon_{Si}/C_j$, ε_{Si} is the silicon permitivity and C_j is the junction capacitance [9]) is the depletion width. By plotting $(qn_i w/J_{r0})$ versus $\exp(qV/2kT)$, as shown in Fig. 6, τ_r and τ_g can be obtained from the slope and intercept of the experimental data, respectively. The recombination lifetime of 4.7 μs was found. It is obvious, that lifetime obtained by this procedure response to low-level carrier injection, which is in excellent agreement with that acquire from OCVD technique (4.5 μs).

Moreover, we realized appropriate simulation of *I-V* characteristic, where as input parameters simulated concentration profile from Fig. 4 and as measured lifetimes were used. Recombination current was solved by SRH model with single dominant level assuming that energy of trap is located at mid-gap $E_T=E_i$. Simulated *I-V* characteristic is shown in Fig. 5 (drown by solid line) and one can conclude good matching between simulated and experimental data. Note that we did not make any additional fitting procedures. Some discrepancies could arise from weak accuracy of

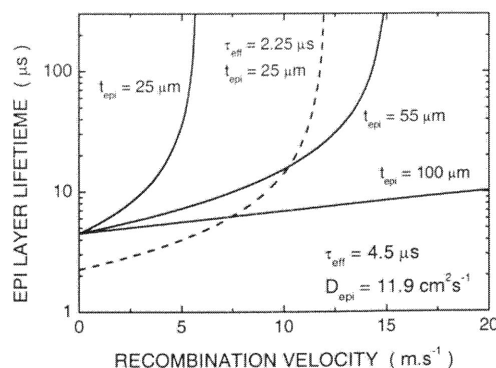

Fig. 7. Epi layer lifetime versus s_r as a function of layer thickness for as measured effective lifetime τ_{eff}=4.5 μs.

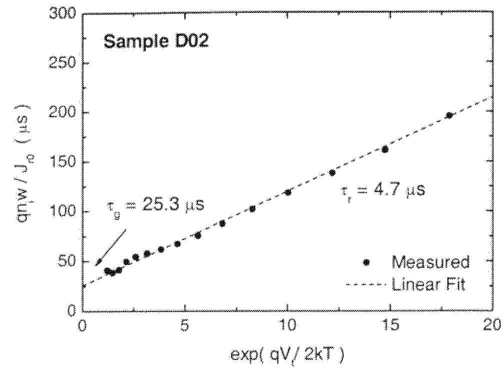

Fig. 6. Extraction of recombination and generation lifetime from I-V and C-V experimental data of the sample D02.

spreading resistance profiling measurement and/or from low-level lifetime extraction.

How can be evaluated τ_{epi}? Fig. 7 shows (solid lines) correlation between τ_{epi} and s_r for given τ_{eff}=4.5μs and epi layer thickness calculated according to egns. (10) and (11). It demonstrates, that with epi thickness decreasing, influence of interface recombination becomes more significant. Now, consider structure with t_{epi}=25 μm and approximately equal epi layer parameters (the same process condition). One can expect the lower value of τ_{eff}, for example, we assume τ_{eff}=2.25 μs. This calculation is drown in Fig. 7 by dash line. Since the minority excess carrier concentration is uniform trough the epi base (t_{epi}<<L_n), s_r is equal for both structures. Only one entity that change with τ_{eff} decreasing in right side of egn. (10) is β, consequently, solution is represents by intersection of solid (t_{epi}=55 μm) and dash line in Fig. 7, resulting τ_{epi}=16.3 μs and s_r=10.25 m/s.

Although, it is only consideration, manufacturing of structures with t_{epi}=25 μm is under process.

Acknowledgement

This work was supported by Slovak Grant Agency project No. 1/0169/03 and APVT 20/0139/02.

REFERENCES

[1] Gossick B.R.: Phys. Rev. 1953; 91: 1012–1013.
[2] Lee S.J., Schroder D.K. Solid-St Electron. 1999; 43(1): 103–111.
[3] Schroder D.K. *et al.* IEEE Trans. Electron Dev. 2003; 50(4): 906–912.
[4] Schroder D.K. Semiconductors material and devices characterization, New York: Wiley-Interscience, 1998.
[5] Ghandhi S.K. Power Semiconductor Devices. New York: Wiley, 1977.
[6] Basset R.J., Fulop W., Hogarth C.A. Int. J. Electron., 1973; 35(2): 177–192.
[7] Ogita Y.I. J. Appl. Phys., 1996; 79: 6954–6960.
[8] Choo S.C., Mazur R.G. Solid-St Electron. 1970; 13(5): 553–564.
[9] Poyai A. *et al.* Material Science Eng. 2003; B102: 189–192.